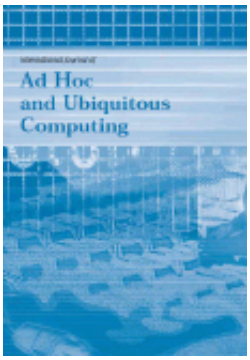

International Journal of Ad Hoc and Ubiquitous Computing

ISSN online: 1743-8233 - ISSN print: 1743-8225
https://www.inderscience.com/ijahuc

Intelligent omni-surfaces with hybrid solar and wind energy harvesting

Faisal Alanazi

DOI: 10.1504/IJAHUC.2024.10066964

Article History:

Received:	29 May 2024
Last revised:	23 July 2024
Accepted:	01 August 2024
Published online:	30 December 2024

Intelligent omni-surfaces with hybrid solar and wind energy harvesting

Faisal Alanazi

Electrical Engineering Department,
College of Engineering,
Prince Sattam Bin Abdulaziz University,
Alkharj, Saudi Arabia
Email: faisal.alanazi@psau.edu.sa

Abstract: This paper studies the throughput of intelligent omni-surfaces (IOS) when the source recovers power from the sun and wind to broadcast packets to two users U_t and U_r. U_t and U_r are located in the transmit and reflect spaces of IOS. The recovered power from the sun depends on radiation intensity that has a Gaussian distribution. IOS is an excellent candidate for 6G communications as it offers significant performance enhancement. However, IOS using the wind or the solar powers was not yet studied. The harvesting process is optimised to maximise the throughput. IOS with 64 elements offers 48 dB gain.

Keywords: intelligent omni-surfaces; IOS; solar; wind energy harvesting; SINR; Rayleigh channels.

Reference to this paper should be made as follows: Alanazi, F. (2025) 'Intelligent omni-surfaces with hybrid solar and wind energy harvesting', *Int. J. Ad Hoc and Ubiquitous Computing*, Vol. 48, No. 1, pp.13–18.

Biographical notes: Faisal Alanazi received his BSc in Electrical Engineering-Communication and Electronics from KSU in 2010 and MSc and PhD in Electrical and Computer Engineering from The Ohio State University in 2013 and 2018, respectively. He is currently working as an Associate Professor at PSAU. His research interests span cryptography, vehicular adhoc networks, delay tolerant networks. He is a member of the IEEE Communication Society.

1 Introduction

IOS transmits packets to two users U_r and U_t in the reflect and transmit spaces of IOS (El-Refay et al., 2023; Vinothini et al., 2023; Zhang et al., 2022a, 2022b; Zhang and Di, 2022). IOS phases are optimised to maximise the SINR and allow a large throughput (Xu et al., 2022; Zhang et al., 2022c; Fang et al., 2022; Chen et al., 2022; Zeng et al., 2022; Wang et al., 2022). Coding techniques for IOS were presented in Zhang et al. (2022a). IOS for unmanned aerial vehicles (UAV) systems was considered in Liu et al. (2022) and Wang et al. (2021). Performance analysis of IOS was presented in Cai et al. (2023), Benaya et al. (2023) and Adhikary et al. (2023). IOS using NOMA was suggested in Adhikary et al. (2023), Cai et al. (2021) and Zhang et al. (2023, 2022b). The security of 6G wireless systems has been improved using IOS in Asif et al. (2024). IOS using cooperative beamforming has been suggested in Zhang et al. (2024a). Spectrum sensing enhancement using IOS has been proposed in Zhang et al. (2024b). The spectral efficiency of IOS with channel estimation errors has been studied in Li et al. (2024). The study takes into account hardware impairments. IOS with energy harvesting using solar, wind or radio frequency signals has not been yet studied and all previous results assume that the source has a chargeable battery. IOS using wind or solar energies was not studied in El-Refay et al. (2023), Vinothini et al. (2023), Zhang et al. (2022a, 2022b), Zhang and Di (2022), Xu et al. (2022), Zhang et al. (2022c), Fang et al. (2022), Chen et al. (2022), Zeng et al. (2022), Wang et al. (2022), Zhang et al. (2022a), Liu et al. (2022), Wang et al. (2021), Cai et al. (2023), Benaya et al. (2023), Adhikary et al. (2023), Cai et al. (2021), Zhang et al. (2023), Zhang et al. (2022b), Asif et al. (2024), Zhang et al. (2024a, 2024b) and Li et al. (2024). In this article, we evaluate the throughput of IOS when the source recovers power from wind and the sun using a photo-voltaic (PV) system. We derive the SINR statistics to deduce the throughput when the source uses IOS and recovers power from wind signals and the sun. IOS is an excellent candidate for 6G communications as it offers significant performance enhancement. However, IOS using the wind or the solar powers was not yet studied. The harvesting process is optimised to maximise the throughput. IOS with 64 elements offers 48 dB gain. Section 2 derives the throughput when IOS uses both solar energy and wind signals. Section 3 gives the results. Section 4 is the conclusion.

2 IOS with solar and wind energy harvesting

In Figure 1, the source S recovers energy from wind and the sun to broadcast a signal to two users U_r and U_t. An IOS is from the source S and U_r, U_t. The transmit and reflect coefficient are $\chi_n^t e^{j\theta_n^t}$ and $\chi_n^r e^{j\theta_n^r}$ wit $0 < \theta_n^t, \theta_n^r < 1$ and $0 < \chi_n^r < 1$, $0 < \chi_n^t < 1$ with $(\chi_n^r)^2 + (\chi_n^t)^2 = 1$. U_r and U_t are located respectively in the space of reflection and transmission of IOS. The channel from S to n-th IOS is $f_n = |f_n|e^{j\phi_{f_n}}$. The channel from n-th IOS and user U_p for $p = t, r$ is $t_n^p = |t_n^p|e^{j\phi_{t_n^p}}$.

The received signal at U_p $p = r, t$ is written as

$$y_p = \sqrt{E_s\zeta_p}\sum_{n=1}^{N} t_n^p\chi_n^p e^{j\theta_n^p} f_n x_p + \sqrt{E_s\zeta_{p'}}\sum_{n=1}^{N} t_n^q\chi_n^q e^{j\theta_n^q} f_n x_{p'} + n_p \quad (1)$$

where E_s is the symbol energy, ζ_p and $\zeta_{p'}$ are power coefficients for U_p and $U_{p'}$ with $\zeta_p + \zeta_{p'} = 1$. x_p (respectively $x_{p'}$) is U_p symbol (respectively $U_{p'}$).

Figure 1 IOS with wind and solar energy harvesting (see online version for colours)

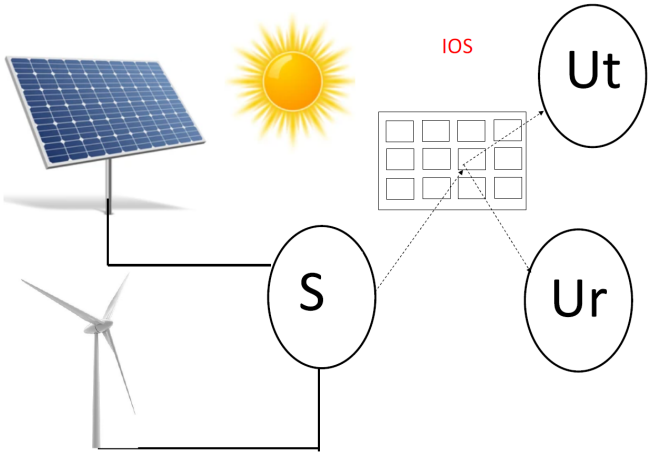

The SINR at U_p is

$$\gamma_p = \frac{E_s\zeta_p W}{N_0 + E_s\zeta_{p'} W} \quad (2)$$

where

$$W = \left|\sum_{n=1}^{N} t_n^p||f_n|\chi_n^p \exp(j[\theta_n^p + \phi_{f_n} + \phi_{t_n^p}])\right|^2 \quad (3)$$

IOS phase shift is

$$\theta_n^p = -\phi_{f_n} - \phi_{t_n^p}. \quad (4)$$

The SINR at U_p is

$$\gamma_p = \frac{E_s\zeta_p A_p^2}{E_s\zeta_{p'} A_{p'}^2 + N_0} \quad (5)$$

where

$$A_p = \sum_{n=1}^{N} |t_n^p||f_n|\chi_n^q \quad (6)$$

A_p is Gaussian with mean $m_{A^p} = \sum_{n=1}^{N} \frac{\pi}{4}\chi_n^p \frac{1}{d_{S,IOS}^{0.5pla} d_{IOS,U_p}^{0.5pla}}$ and variance $\sigma_{A_p}^2 = \sum_{n=1}^{N}[1 - \frac{\pi^2}{16}](\chi_n^p)^2 \frac{1}{d_{S,IOS}^{pla} d_{IOS,U_p}^{pla}}$ where pla is the path loss attenuation and d_{XY} is the distance between X and Y.

Let $X_p = A_p^2$ and $Y_p = E_s X_p$, the CDF of γ_p is equal to

$$F_{\gamma_p}(x) = F_{Y_p}\left(\frac{N_0 x}{\zeta_p - \zeta_{p'} x}\right). \quad (7)$$

where $F_{Y_p}(x)$ is provided in Subsection 2.3.

2.1 Solar energy harvesting model

The recovered power P in S is written as

$$P^{solar} = \eta RI(t), \quad (8)$$

with $0 < \eta < 1$ and

$$RI(t) = RI_1(t) + RI_2(t), \quad (9)$$

where

$$I_1(t) = \begin{cases} I_{MAX}(\frac{2t}{3} - 3 - \frac{t^2}{36}) = 0 \text{ otherwise} \end{cases} \quad (10)$$

$I_2(t)$ has a Gaussian distribution expressed as

$$f_R I(y) = \frac{1}{\sqrt{2\pi A^2}} \exp\left(-\frac{[y - RI_1(t)]^2}{2A^2}\right) \quad (11)$$

Let $0 < \alpha < 1$ be the harvesting time and T is frame length, the recovered power during αT seconds is expressed as:

$$E^{solar} = \alpha T P^{solar}. \quad (12)$$

The symbol energy E_s^{solar} obtained from sun is

$$E_s^{solar} = \frac{T_s RI(t)\alpha\eta}{1 - \alpha}. \quad (13)$$

where T_s is the symbol duration. The PDF of E_s^{solar} is

$$f_{E_s^{solar}}(y) = \frac{1}{\sqrt{2\pi\sigma^2}} \exp\left(-\frac{[y - M(t)]^2}{2\sigma^2}\right), \quad (14)$$

with

$$M(t) = \frac{RI_1(t)\alpha\eta T_s}{1 - \alpha} \quad (15)$$

$$\sigma^2 = \frac{T_s^2 A^2 \alpha^2 \eta^2}{(1 + \alpha^2 - 2\alpha)} \quad (16)$$

2.2 Wind energy harvesting

The wind speed V follows a Weibull distribution given by

$$f_V(v) = \left(\frac{v}{c}\right)^{k-1} \frac{k}{c} e^{-(\frac{v}{c})^k}, \tag{17}$$

where

$$k = \left(\frac{\sigma}{\mu}\right)^{-1.086} \tag{18}$$

$$c = \frac{\mu}{\Gamma\left(1+\frac{1}{k}\right)}, \tag{19}$$

σ and μ are the standard deviation and mean of wind speed..

The CDF of V is

$$F_V(v) = 1 - e^{-(\frac{v}{c})^k}. \tag{20}$$

c is the wind strength at the and k is the peak value.

The recovered power P from wind is expressed as (Vinothini et al., 2023)

$$P^{wind} = 0.5\rho A C v^3, \tag{21}$$

where $A = \pi r^2$, r is the rotor radius, C is a power coefficient and ρ is the density of air.

The recovered energy at S during αT seconds is

$$E^{wind} = \alpha T P^{wind}. \tag{22}$$

The symbol energy E_s^{wind} recovered from wind at S is written as

$$\begin{aligned} E_s^{wind} &= \frac{E^{wind}}{\frac{(1-\alpha)T}{T_s}} = \frac{\alpha T P^{wind}}{\frac{(1-\alpha)T}{T_s}} \\ &= \frac{\alpha T_s P^{wind}}{1-\alpha} = \Delta v^3, \end{aligned} \tag{23}$$

where

$$\Delta = \frac{\alpha T_s \rho A C}{2(1-\alpha)}. \tag{24}$$

The CDF of E_s^{wind} is

$$\begin{aligned} F_{E_s^{wind}}(x) &= P(\Delta v^3 \le x) \\ &= 1 - e^{-(\frac{x}{\Delta})^{\frac{k}{3}} \frac{1}{c^k}} \\ &= 1 - e^{-(\frac{2x(1-\alpha)}{\alpha T_s \rho A C})^{\frac{k}{3}} \frac{1}{c^k}}. \end{aligned} \tag{25}$$

The PDF of E_s^{wind} is equal to

$$f_{E_s^{wind}}(x) = \frac{k}{3} \beta x^{\frac{k}{3}-1} e^{-\beta x^{\frac{k}{3}}} \tag{26}$$

where $\beta = (\frac{2(1-\alpha)}{\alpha T_s \rho A C})^{\frac{k}{3}} \frac{1}{c^k}$.

The total available symbol energy is the sum of energies recovered from sun and wind

$$E_s = E_s^{wind} + E_s^{solar} \tag{27}$$

As E_s^{wind} and E_s^{solar} are independent, the PDF of E_s is equal to

$$f_{E_s}(x) = (f_{E_s^{solar}} * f_{E_s^{wind}})(x), \tag{28}$$

where $*$ is the convolution operator.

2.3 Y_q statistics

The variable Y_q is given by

$$Y_q = E_s X_q \tag{29}$$

where

$$X_q = A_q^2, \tag{30}$$

We have (Li et al., 2024)

$$\begin{aligned} F_{X_q}(y) &= P\left(|A_q| \le \sqrt{y}\right) \\ &\simeq 0.5 erfc\left(\frac{-\sqrt{y} - m_{A_q}}{\sqrt{2}\sigma_{A_q}}\right) \\ &\quad - 0.5 erfc\left(\frac{\sqrt{y} - m_{A_q}}{\sqrt{2}\sigma_{A_q}}\right) \end{aligned} \tag{31}$$

The CDF of the Y_q is:

$$\begin{aligned} F_{Y_q}(x) &= \int_0^{+\infty} f_{E_s}(y) F_{X_q}\left(\frac{x}{y}\right) dy \\ &\simeq \frac{1}{2\sqrt{2\pi\sigma^2}} \int_0^{+\infty} \exp\left(-\frac{[y - M(t)]^2}{2\sigma^2}\right) \\ &\quad erfc\left(\frac{-\sqrt{\frac{x}{y}} - m_{A_q}}{\sqrt{2}\sigma_{A_q}}\right) \\ &\quad - \frac{1}{2\sqrt{2\pi\sigma^2}} \int_0^{+\infty} \exp\left(-\frac{[y - M(t)]^2}{2\sigma^2}\right) \\ &\quad erfc\left(\frac{\sqrt{\frac{x}{y}} - m_{A_q}}{\sqrt{2}\sigma_{A_q}}\right) dy \end{aligned} \tag{32}$$

The packet error probability (PEP) is equal to (Xi et al., 2011)

$$PEP_q(\alpha) < F_{\gamma_q}(W), \tag{33}$$

where (Xi et al., 2011)

$$\begin{aligned} W &= \int_0^{+\infty} 1 \\ &\quad - \left[1 - \left(1 - \frac{1}{\sqrt{M}}\right) Q\left(\sqrt{\frac{3y}{M-1}}\right)\right]^L dy, \end{aligned} \tag{34}$$

where L and M are packet and constellation size.

The throughput is

$$\begin{aligned} Thr_q(\alpha) &= [1-\alpha][1 - PEP_q(\alpha)] \\ &> [1-\alpha][1 - F_{\gamma_q}(W)] \end{aligned} \tag{35}$$

The throughput is optimised as follows

$$Thr_q^{\max} = \max_{0<\alpha<1} Thr_q(\alpha). \tag{36}$$

Figure 2 Throughput of hybrid energy harvesting for $N = 8$ (see online version for colours)

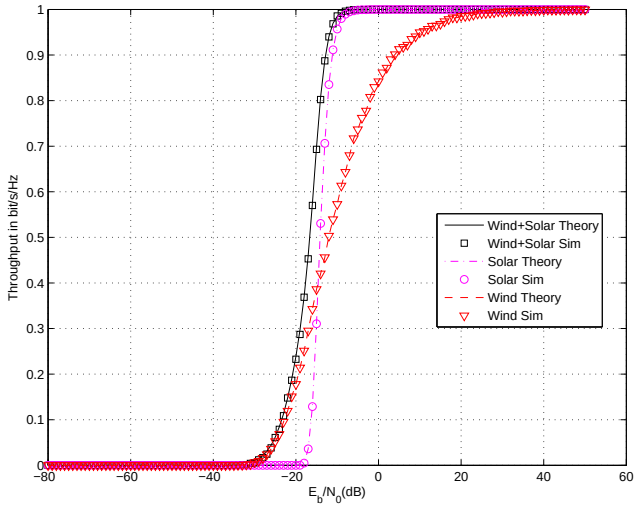

Figure 3 Throughput of hybrid energy harvesting for $N = 16$ (see online version for colours)

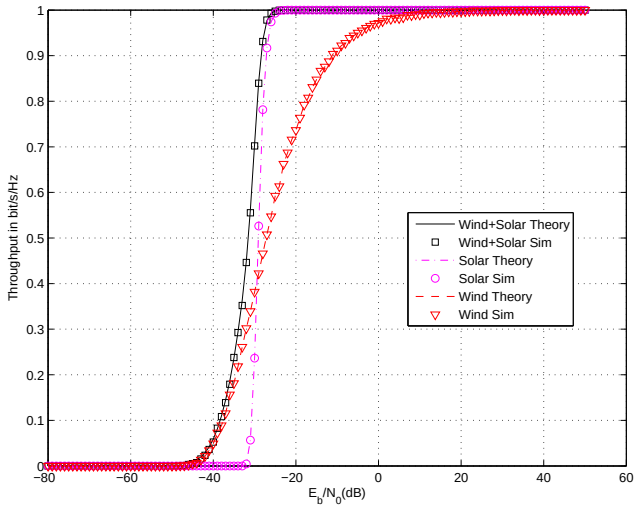

Figure 4 Throughput of hybrid energy harvesting for $N = 32$ (see online version for colours)

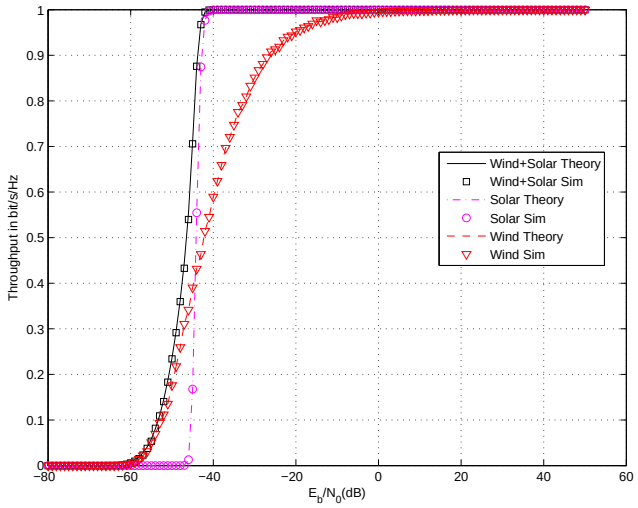

Figure 5 Throughput of hybrid energy harvesting for $N = 64$ (see online version for colours)

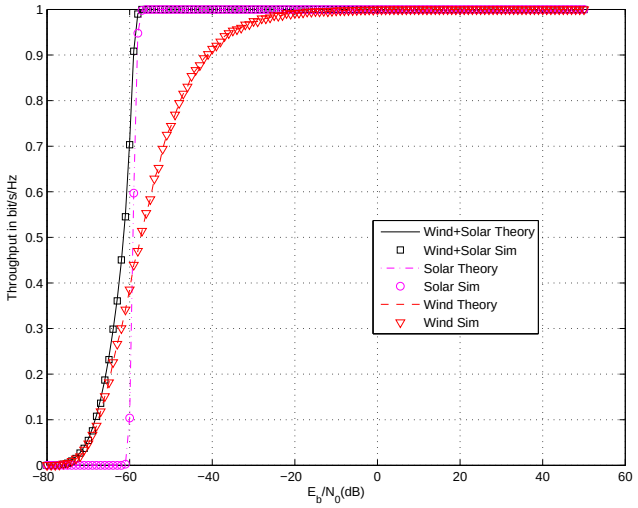

Figure 6 Throughput of IOS using wind and solar energies for $N = 8, 16, 32, 64$ (see online version for colours)

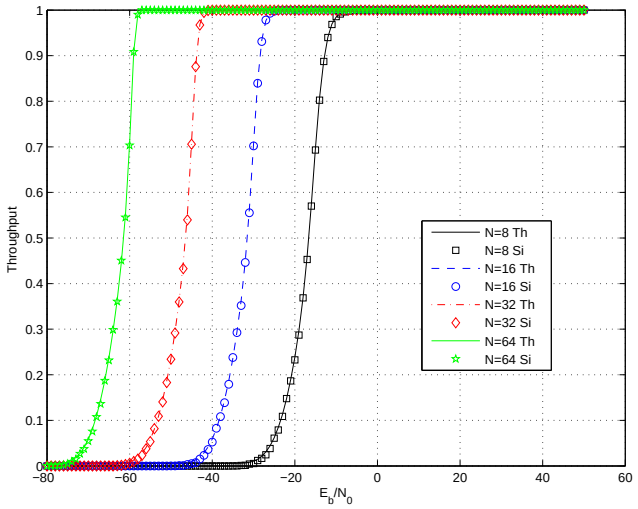

Figure 7 Throughput of IOS using solar energy for $N = 8, 16, 32, 64$ (see online version for colours)

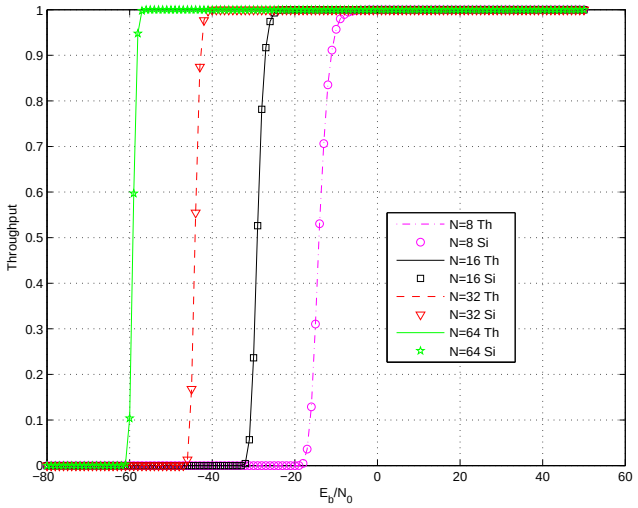

3 Numerical results

The used parameters are $\eta = 0.2$, $\beta = 0.5$, $E_N = 1$, $d_{S,IOS} = 1$, $d_{IOS,U_t} = 1$, $d_{IOS,U_r} = 1.5$, $d_{N,S} = 0.5$, $L = 500$, $ple = 3$, $a = 1$, $I_{\max} = 20$ and $t = 12$. The other parameters are $\zeta_q = 0.8 = 1 - \zeta_{q'}$ $\eta_n^t = \eta_n^r = \frac{1}{\sqrt{2}}$.

Figure 8 Throughput of IOS using wind for $N = 8, 16, 32, 64$ (see online version for colours)

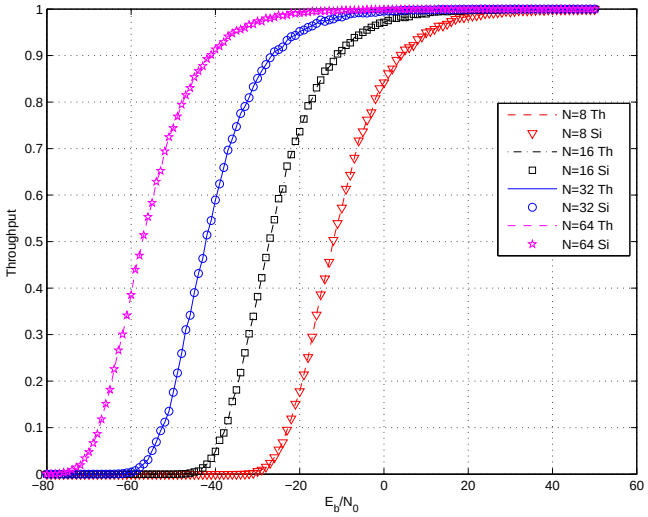

Figures 2–5 show the throughput for $t = 12$, $\alpha = 0.5$ and QPSK modulation and $N = 8, 16, 32, 64$. Hybrid energy harvesting a higher throughput than using only the wind or solar energy. Figures 6–8 show that IOS with 64 elements allows 48 dB gain. These results are valid for both hybrid, solar and wind energy harvesting.

4 Conclusions

In this article, we evaluated the throughput of IOS if the source recovers power from the wind and the sun using a PV system. The recovered power is used by the source to broadcast data to users U_t and U_r. IOS phases were optimised to maximise the SINR. IOS with 64 elements allows 48 dB gain. As a perspective, we can study IOS using non-orthogonal multiple access (NOMA). In fact, NOMA will enhance the throughput of IOS since the symbols of many users can be transmitted jointly using optimised power coefficients.

References

Adhikary, A., Munir, M.S., Raha, A.D., Qiao, Y., Hong, S.H., Huh, E-N. and Hong, C.S. (2023) 'An artificial intelligence framework for holographic beamforming: coexistence of holographic MIMO and intelligent omni-surface', *2023 International Conference on Information Networking (ICOIN)*.

Asif, M., Bao, X., Ihsan, A., Khan, W.U., Ahmed, M. and Li, X. (2024) 'Securing NOMA 6G communications leveraging intelligent omni-surfaces under residual hardware impairments', *IEEE Internet of Things Journal*, Vol. 11, No. 14, pp.25326–25336.

Benaya, A.M., Ismail, M.H., Ibrahim, A.S. and Salem, A.A. (2023) 'Physical layer security enhancement via intelligent omni-surfaces and UAV-friendly jamming', *IEEE Access*, Vol. 11, pp.2531–2544.

Cai, W., Liu, R., Liu, Y., Li, M. and Liu, Q. (2021) 'Joint beamforming designs for intelligent omni surface assisted wireless communication systems', *2021 IEEE Global Communications Conference (GLOBECOM)*.

Cai, W., Li, M., Liu, Y., Wu, Q. and Liu, Q. (2023) 'Joint beamforming design for intelligent omni surface assisted wireless communication systems', *IEEE Transactions on Wireless Communications*, Vol. 22, No. 2, pp.101–110.

Chen, Y., Wang, Y., Wang, Z. and Zhang, P. (2022) 'Robust beamforming for active reconfigurable intelligent omni-surface in vehicular communications', *IEEE Journal on Selected Areas in Communications*, Vol. 40, No. 10, pp.3086–3103.

El-Refay, E.A., Malhat, H.A., Zainud-Deen, S.H. and Badawy, M.M. (2023) 'Plasma-based intelligent omni-surfaces', *2023 40th National Radio Science Conference (NRSC)*.

Fang, S., Chen, G., Abdullah, Z. and Li, Y. (2022) 'Intelligent omni surface-assisted secure MIMO communication networks with artificial noise', *IEEE Communications Letters*, Vol. 26, No. 6, pp.2200–2209.

Li, Q., El-Hajjar, M. and Hanzo, L. (2024) 'Ergodic spectral efficiency analysis of intelligent omni-surface aided systems suffering from imperfect CSI and hardware impairments', *IEEE Transactions on Communications*, August, Vol. 72, No. 8, pp.5073–5086.

Liu, Y., Duo, B., Wu, Q., Yuan, X. and Li, Y. (2022) 'Full-dimensional rate enhancement for UAV-enabled communications via intelligent omni-surface', *IEEE Wireless Communications Letters*, Vol. 11, No. 9, pp.1955–1959.

Vinothini, N., Prabha, S.B.D., Fathima, D., Saktheeswaran, A. and Ananthi, G. (2023) 'Intelligent omni surface assisted wireless information and power transfer', *2023 International Conference on Microwave, Optical, and Communication Engineering (ICMOCE)*.

Wang, W., Ni, W. and Tian, H. (2021) 'Securing aerial offloading via intelligent omni-surface', *2021 IEEE Globecom Workshops (GC Wkshps)*.

Wang, W., Ni, W., Tian, H. and Song, L. (2022) 'Intelligent omni-surface enhanced aerial secure offloading', *IEEE Transactions on Vehicular Technology*, Vol. 71, No. 5, pp.5007–5022.

Xi, Y., Burr, A., Wei, J.B. and Grace, D. (2011) 'A general upper bound to evaluate packet error rate over quasi-static fading channels', *IEEE Trans. Wireless Communications*, May, Vol. 10, No. 5, pp.1373–1377.

Xu, J., Liu, Y., Mu, X., Zhou, J.T., Song, L., Poor, H.V. and Hanzo, L. (2022) 'Simultaneously transmitting and reflecting intelligent omni-surfaces: modeling and implementation', *IEEE Vehicular Technology Magazine*, Vol. 17, No. 2, pp.46–54.

Zeng, S., Zhang, H., Di, B., Liu, Y., Di Renzo, M., Han, Z., Poor, H.V. and Song, L. (2022) 'Intelligent omni-surfaces: reflection-refraction circuit model, full-dimensional beamforming, and system implementation', *IEEE Transactions on Communications*, Vol. 70, No. 11, pp.7711–7727.

Zhang, H. and Di, B. (2022) 'Intelligent omni-surfaces: simultaneous refraction and reflection for full-dimensional wireless communications', *IEEE Communications Surveys and Tutorials*, Vol. 24, No. 4, pp.1997–2028.

Zhang, Y., Di, B., Zhang, H., Dong, M., Yang, L. and Song, L. (2022a) 'Dual codebook design for intelligent omni-surface aided communications', *IEEE Transactions on Wireless Communications*, Vol. 21, No. 11, pp.39–45.

Zhang, Y., Di, B., Zhang, H., Dong, M., Yang, L. and Song, L. (2022b) 'Codebook design and beam training for intelligent omni-surface aided communications', *2022 IEEE Wireless Communications and Networking Conference (WCNC)*, pp.219–233.

Zhang, Y., Di, B., Zhang, H., Han, Z., Poor, H.V. and Song, L. (2022c) 'Meta-wall: intelligent omni-surfaces aided multi-cell MIMO communications', *IEEE Transactions on Wireless Communications*, Vol. 21, No. 9, pp.7026–7039.

Zhang, S., Zhang, H., Di, B., Tan, Y., Di Renzo, M., Han, Z., Poor, H.V. and Song, L. (2022a) 'Intelligent omni-surfaces: ubiquitous wireless transmission by reflective-refractive metasurfaces', *IEEE Transactions on Wireless Communications*, Vol. 21, No. 1.

Zhang, H., Zeng, S., Di, B., Tan, Y., Di Renzo, M., Debbah, M., Han, Z., Poor, H.V. and Song, L. (2022b) 'Intelligent omni-surfaces for full-dimensional wireless communications: principles, technology, and implementation', *IEEE Communications Magazine*, Vol. 60, No. 2, pp.9232–9245.

Zhang, Z., Sun, Q., Zhang, J., Ng, D.W.K. and Ai, B. (2023) 'Ergodic capacity of intelligent omni-surface-aided communication systems with phase quantization errors and outdated CSI', *IEEE Systems Journal*, Vol. 17, No. 2, pp.1889–1898.

Zhang, H., Zhu, Y. and Xu, Z. (2024a) 'Intelligent omni-surfaces aided cell-free networks: cooperative beamforming with coupled phase-shift', *IEEE Transactions on Vehicular Technology*, pp.1–6.

Zhang, Z., Chen, W., Wu, Q., Li, Z., Zhu, X. and Yuan, J. (2024b) 'Intelligent omni surfaces assisted integrated multi-target sensing and multi-user MIMO communications', *IEEE Transactions on Communications*, August, Vol. 72, No. 8, pp.4591–4606.